agriculture

MDPI

Article

Characteristics of Dissolved Organic Matter (DOM) Combined with As in Fe-Rich Red Soils of Tea Plantations in the Southern Anhui Province, East China

Youru Yao [1,†], Juying Li [2,†], Kang Ma [1], Jingyi Zhang [1], Yuesheng Lin [1], Huarong Tan [1], Jia Yu [2,*] and Fengman Fang [1,*]

[1] Key Laboratory of Earth Surface Processes and Regional Response in the Yangtze-Huaihe River Basin, Anhui Province, School of Geography and Tourism, Anhui Normal University, Wuhu 241002, China; yaoyouru@ahnu.edu.cn (Y.Y.); 1921011181@ahnu.edu.cn (K.M.); zjyahnu0115@ahnu.edu.cn (J.Z.); ys1213@ahnu.edu.cn (Y.L.); tanhr@ahnu.edu.cn (H.T.)

[2] Nanjing Institute of Environmental Science, Ministry of Ecology and Environment, Nanjing 210042, China; lijuying@nies.org

* Correspondence: yujia@nies.org (J.Y.); ffm1974@mail.ahnu.edu.cn (F.F.); Tel.: +86-157-2062-0961 (J.Y.); +86-153-7568-7225 (F.F.)

† These authors contributed equally to this work.

Abstract: Dissolved organic matter (DOM) is widely present in soil environments and plays a crucial role in controlling the morphology, environmental behavior, and hazards of arsenic (As) in soil. In the Fe-rich red soil of tea plantations, the decomposition of tea tree litter complicates DOM properties, leading to more uncertain interactions between DOM, Fe, and As. This study focused on three tea plantations in Huangshan City to investigate the contents of DOM, Fe, and As in surface red soils (*Ferralsols*) and establish their correlations. Three-dimensional fluorescence spectroscopy and PARAFAC analysis methods were used to analyze the DOM components and fluorescence signatures. Additionally, the process and mechanism of the binding of DOM-Fe with As were explored through laboratory experiments on the morphological transformation of As by DOM-Fe. The results showed that the pH values of the soils in the three tea plantations ranged from 3.9 to 5.2, and the entire sample was strongly acidic. The DOM exhibited strong intrinsic properties and low humification, containing three types of humic acid components and one intermediate protein component. The DOC content in the Fe-rich red soil did not have a direct correlation with Fe and As, but the interaction of DOM fractions with Fe significantly influenced the As content. Specifically, the interaction of protein-like fractions with Fe had a more pronounced effect on the As content. The maximum sorption rate of As by DOM was 15.45%, and this rate increased by 49 to 75% with the participation of Fe. In the configuration of the metal electron bridge, Fe acts as a cation, forming a connecting channel between the negatively charged DOM and As, thus enhancing the DOM's binding capacity to As. DOM-Fe compounds bind As through surface pores and functional groups. These findings provide deeper insights into the influence of DOM on As behavior in Fe-rich soil environments and offer theoretical support for controlling As pollution in red soil.

Keywords: dissolved organic matter; arsenic; iron; combination; Anhui province

Citation: Yao, Y.; Li, J.; Ma, K.; Zhang, J.; Lin, Y.; Tan, H.; Yu, J.; Fang, F. Characteristics of Dissolved Organic Matter (DOM) Combined with As in Fe-Rich Red Soils of Tea Plantations in the Southern Anhui Province, East China. *Agriculture* **2024**, *14*, 2289. https://doi.org/10.3390/agriculture14122289

Academic Editor: Alvyra Šlepetienė

Received: 12 November 2024
Revised: 9 December 2024
Accepted: 11 December 2024
Published: 13 December 2024

1. Introduction

Arsenic (As) is a highly toxic element known for its nerve toxicity, teratogenicity, and strong carcinogenic properties, causing acute and chronic damage to the cardiovascular, digestive, and nervous systems, ultimately leading to cancer. This has become a global environmental and public health issue [1,2]. Over the past few decades, China has rapidly evolved into the world's largest industrial and agricultural powerhouse; however, extensive industrial and agricultural activities have released significant amounts of As into the soil [3]. This has resulted in varying degrees of As pollution nationwide, particularly in agricultural

soils due to the use of As-containing pesticides and fertilizers, exacerbating the pollution situation [4–6]. The excessive accumulation of As in agricultural soils not only reduces the crop yield and quality, threatening food supply and safety but also, due to its non-biodegradability and biological nature, allows As to enter the human body through the food chain, leading to diseases and an increase in public health burdens [7,8]. The toxicity and mobility of As are closely linked to its chemical forms, primarily existing in inorganic forms such as arsenite (As(III)) and arsenate (As(V)). The toxicity and migration potential of As(III) are significantly greater than those of As(V) [9]. However, under specific conditions such as pH, redox state, the presence of Fe/Mn minerals, and organic matter presence, As(III) and As(V) can transform into one another, impacting their biotoxicity and transport capacities [10].

Dissolved organic matter (DOM), which mainly includes fulvic acid, humic acid (HA) (under alkaline conditions), small molecule organic matter, and microbial metabolites, significantly influences the biogeochemical behavior of As [11,12]. The DOM serves as an energy source for soil microorganisms and has a significant intrinsic negative charge, enabling it to function as an effective electron donor or acceptor. This property allows the DOM to interact with As, thereby exerting a substantial influence on its environmental behavior in soil [11,13]. Previous studies have demonstrated a strong correlation between DOM content and As concentrations in soil [14]. However, the DOM content alone does not fully determine As mobility; the specific properties of DOM also play a major role in its binding affinity for As [15,16]. DOM derived from different sources (e.g., externally introduced DOM and DOM produced by microbial decomposition), fractions (such as Ultrafilter Retained OM (>1000 Da) and Ultrafilter Retained OM (<1000 Da)), and those with varying structural characteristics (e.g., aromaticity, hydrophobicity) exhibit varying binding processes and efficiencies for As [17,18]. For instance, fulvic acid can adsorb onto soil particle surfaces, increasing their negative charge and promoting As desorption by reducing the competitive sorption of other anions [19]. HA, under alkaline conditions, can dissolve and contribute to the DOM pool, forming DOM-As complexes via sorption and complexation, which can enhance As mobility [20]. Furthermore, Fe acts as a key mediator between DOM and As by forming ternary complexes (DOM-Fe-As) through metal-bridging bonds. These complexes accelerate the mechanical dispersion and molecular diffusion of As in porous media, thereby increasing its migration rate [21–23]. Despite these findings, the interactions between DOM and As in Fe-rich soil environments remain poorly understood, necessitating further investigation.

Tea plantation soils in southern China provide an ideal setting to examine the relationship and binding characteristics among Fe, DOM, and As, as Fe-rich red soils are a key resource in these regions. The global issue of As contamination in agricultural soils has raised concerns among producers and consumers regarding As levels in tea [23], an important indicator for evaluating tea quality [24]. Huangshan City in the Anhui Province, a major tea-producing area, features typical subtropical tea gardens with red soil and hills. Studies indicate that the average As content in the soil of tea areas in the South Anhui Province is 16.35 ± 30.69 mg·kg^{-1}, exhibiting notable spatial variation [25]. Moreover, to maintain soil fertility in tea plantations, the decomposing leaves of tea trees are mulched on the soil surface, enhancing the soil organic matter content. This annual mulching alters the surface soil environment, inducing changes in DOM properties during organic matter decomposition and creating uncertainties in DOM-As binding within Fe-rich red soils [26,27]. Thus, further investigations into the binding of DOM to As in the red soils of tea plantations will provide insights into the complex chemical behavior of As in Fe-rich soil environments.

In this study, the surface red soils from three tea gardens in Huangshan City, Anhui Province, were selected as the study medium, with As as the target pollutant. This research aimed to investigate the binding characteristics and mechanisms of DOM and As in Fe-rich red soil. The main objectives were: (1) to characterize the content of the dissolved organic matter (DOM), Fe, and As in the red soils of the three tea gardens and compare

the differences; (2) to analyze the correlations among DOM, Fe, and As; and (3) to select a typical DOM and conduct simulation experiments to reveal the binding mechanism of DOM-Fe with As.

2. Materials and Methods

2.1. Study Area

Huangshan City (117°02′–118°55′ E, 29°24′–30°24′ N) is located in the mountainous region of southern Anhui, with elevations ranging from 85 to 1865 m a.s.l. The area is characterized by undulating and complex topography, predominantly mountainous, but also featuring basins, plains, and hills. The region experiences a subtropical humid monsoon climate, with an average annual temperature of 15.5 °C to 16.4 °C and an average annual precipitation of 1816 mm. The climate is typically cloudy and humid, providing ideal conditions for growing tea, fruit trees, and other crops. Tea is one of the main industries in Huangshan City. According to statistics, the city has about 800,000 acres of tea plantations, and in 2022, tea production exceeded 45,000 tons, accounting for one-third of the Anhui Province's total tea output. The total value of the tea industry chain reached 23 billion Yuan. However, industrial and agricultural activities have led to some degree of As contamination in the soil [26]. In 2020, statistics showed that 32.82 million tons of fertilizers, 472.95 million tons of organic fertilizers, and 25,200 tons of pesticides were used in Huangshan City, with fertilizer and pesticide utilization rates both exceeding 40% [26].

2.2. Sample Collection and Pre-Processing

The soils in the sampling area are mainly ferric acrisols [26–28]. They are aluminum-rich acidic soils formed under subtropical evergreen deciduous forests, distributed in areas with obvious changes in dry and wet seasons. The sedimentary layer is reddish-brown or orange-red, and there are reticulated and iron-manganese nodules in the lower part of the profile. The silica/alumina ratio is ~1.9 to 2.2, and the clay minerals include kaolinite, muscovite, and trihydrate aluminum ore [26]. The cation exchange is lower than that of other soil types, ranging from 6 to 121 cmol/kg.

Soil samples were collected from tea gardens in the Huangshan District, Huizhou District, and Qimen County in accordance with the distribution of tea tree species across the city. On a sunny and windless day in June 2022, soil samples from 0–20 cm depth were collected using a stainless steel shovel following the plum blossom sampling method [17]. Stones and dead leaves were removed, and the collected soil was thoroughly mixed. Approximately 500 g of the mixed soil was selected using the quartering method and placed in polyethylene ziplock bags for transport to the laboratory for analysis. A total of 52 surface soil samples were collected: 20 from the Huangshan Maofeng tea production area (HSMF), 16 from the Taiping green tea production area (TPHK), and 16 from the Qimen Black tea production area (QMH). The locations of the sampling points are shown in Figure 1. All tea-producing areas have been utilized for tea-growing activities for a long period of time, and there are no industrial activities other than agricultural cultivation.

The soil samples were placed in a dry and well-ventilated environment for natural air drying. After drying, impurities (mainly gravel, debris, tree branches, and large leaf fragments) were removed from the soil. The air-dried samples were then repeatedly crushed using a heavy weight to pass through a 2.0 mm nylon sieve. Subsequently, the soil was further ground using an agate mortar to pass through a 0.15 mm nylon sieve. The processed soil samples were stored in polyethylene sealed bags for further analysis. All experiments were performed at room temperature (25 °C) unless otherwise noted.

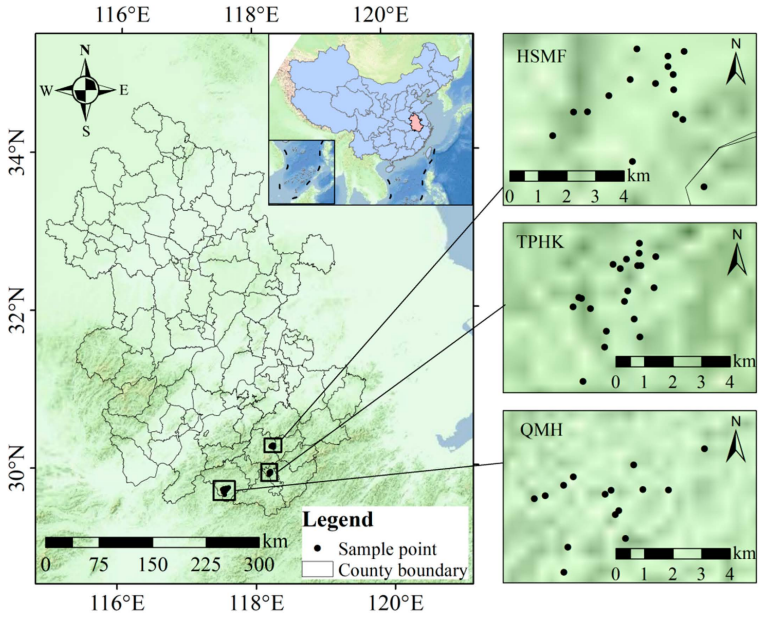

Figure 1. Distribution of the study area and sampling sites.

2.3. Extraction and Characterization of Soil DOM

To extract the DOM, 5 g of the soil samples were dissolved in 50 mL of deionized water (*w*/*v*, 1:10) and subjected to oscillation at room temperature for 24 h. Afterward, the samples were centrifuged at 6000 rpm for 15 min. The supernatant was collected and filtered through a 0.45 µm glass fiber filter membrane to obtain the DOM extract. The extracted DOM was then placed in 250 mL brown glass bottles and stored in a refrigerator at 4 °C in the dark. To avoid any experimental interference from dissolved carbonates in the water, distillation was used to remove dissolved carbonates from the secondary deionization (DI water). The experimental water used for the DOM extraction and DOC determination was heated to boiling with DI water, and then the water was evaporated and collected by condensation.

A TOC analyzer (Vario TOC, Elementar, Hanau, Germany) was used to determine the dissolved organic carbon (DOC) content (analyze DOC content to assess DOM quantity [29]). A fluorescence spectrometer (F97Pro, Prism, Shanghai, China) was used to scan the three-dimensional fluorescence spectral features of the DOM solutions. The fluorescence spectra were scanned in the range of excitation (Ex) from 200 to 450 nm (in 5 nm increments) and emission (Em) from 250 to 550 nm (in 2 nm increments), with a scanning speed of 2400 nm/min, and both Ex and Em slit widths were set to 5 nm. To eliminate the effects of Rayleigh and Raman scattering, ultrapure water was used as a blank control, and the DOM sample spectra were corrected by subtracting the fluorescence spectrum of ultrapure water.

2.4. Determination of Investigated Elements

Strong acids were used to break down the soil matrix and release arsenic into the solution. A quantity of soil (0.5 g) was placed into a Teflon digestion vessel. A mixture of aqua regia (3:1 HCl to HNO_3 ratio) or a combination of concentrated HNO_3 and HCl (about 9 mL 12 M HCl and 3 mL 16 M HNO_3) was added. The vessels were sealed and heated in a microwave digestion system to about 180–200 °C for 20–30 min. After digestion, the solution was filtered through a 0.45 µm filter to remove any remaining solid particles. The filtrate was diluted with deionized water to a final volume of 100 mL to prepare the sample for ICP-MS (NexION 2000, PerkinElmer, Waltham, MA, USA) analysis. For the determination of As concentrations in the compound liquids, the liquids were passed through a 0.22 µm filter membrane, subsequently diluted 10-fold with 2% HNO_3, and measured directly by ICP-MS. For the Fe content, the soil samples were digested with HF-

$HClO_4$-HNO_3. For the Fe content of soil, 0.2 g of the soil sample was accurately weighed into an inner polytetrafluoroethylene crucible, made wet with a few drops of water, then 3 mL of 16 M HNO_3 and 1.0 mL of 22 M HF were added. The mixture was shaken well, and the crucible was placed into a stainless steel sleeve, screwed tightly, and put into the oven at 180 °C for 8 h of ablation. After cooling to room temperature (~25 °C), the inner crucible was removed, the inner wall of the lid was rinsed with water, and it was placed on an electric heating plate at 100–120 °C and heated for about 3 h until about 2–3 mL of solution remained in the crucible. A volume (1 mL) of 12 M $HClO_4$ was added, the temperature was raised to 170 °C, and the mixture was evaporated until thick white smoke was observed. The evaporation continued until it was almost dry, then the inner wall was rinsed with 2% dilute HNO_3, and the solution was condensed into 50 mL. The Fe content was determined using an inductively coupled plasma emission spectrometer (PerkinElmer ICP-OES Optima 7000, USA). Parallel samples were prepared throughout the experiment, and standard solutions were used for calibration during the sample analysis. The relative standard deviation was kept within ±20%.

2.5. Sorption Experiment

Laboratory dialysis experiments were conducted to quantify the binding of As by different DOM-Fe complexes. HA (Shanghai Aladdin Biochemical Science and Technology Co., Ltd., Shanghai, China) (The purification steps and pretreatment details of HA are presented in Text S1 of Supplementary Materials) and $FeSO_4$ were selected as representative DOM and Fe sources, respectively. Different HA solutions (0, 10, 20, 50, and 100 mg·L^{-1}), Fe solutions (0, 1, 5, 10, 20, 30, 40, and 50 mg·L^{-1}), and varying combinations (two-by-two combinations of different concentrations of HA and Fe) of HA and Fe were prepared. The solutions were placed into dialysis bags, which were submerged in a 250 mL brown glass bottle filled with 50 mL of 1 mg·L^{-1} As solution (Na_3AsO_4, As(V)). The bags were fully submerged in the external As solution. The bottle was shaken in a constant temperature shaker for 72 h, and 5 mL of the As solution was collected to measure the As content. The content of As outside the dialysis bag represented the free As content, and the difference between the total As and the free As contents was considered the bound As content.

In another experiment, 200 mg of HA was dissolved in 1 L of deionized water, followed by the addition of 10 mg of Fe(II) to create a DOM-Fe solution. Then, 0.25 mg, 0.5 mg, 2 mg, 5 mg, 10 mg, and 20 mg of As(V) were added to the DOM-Fe solution, which was shaken at 25 °C for two days. The surface morphology of the DOM-Fe before and after As binding was observed using a scanning electron microscope.

2.6. Methods of Analysis

Parallel factor (PARAFAC) analysis identifies the most suitable fluorescence components by pinpointing the peaks of the 3D fluorescence spectra and is a reliable method for analyzing 3D fluorescence spectral data [30]. In this study, the 3D fluorescence spectra of the soil DOM from three tea plantations were analyzed using the DOMFluor and drEEM toolboxes in Matlab R2023b to extract the DOM fluorescence components. The results were validated through split-half testing, residual analysis, and loadings analysis. Additionally, fluorescence information was recorded for all data using maximum fluorescence intensity (Fmax) [31].

The Freundlich isothermal sorption model describes multimolecular layer sorption. The sorption characteristics of DOM-Fe with heavy metals align with the Freundlich isothermal sorption model [32]. Therefore, the sorption of arsenic (As) by the DOM-Fe can be calculated using the Freundlich sorption model. The Freundlich sorption isotherm equation can be expressed as follows:

$$log\ Q_e = log\ K_f + \frac{1}{n} log\ C_e \quad (1)$$

In Equation (1), the amount of equilibrium sorption type is Q_e (mg·g^{-1}), C_e refers to the sorption properties of equilibrium content (mg·g^{-1}), K_f and n refer to the constant Freundlich sorption ability and sorption intensity index, respectively. Its linear form is as follows (Equation (2)):

$$Q_e = K_1 lnK_2 + K_1 lnC_e \quad (2)$$

The Generalized Additive Model (GAM) is based on the Generalized Linear Model (GLM) and extends the nonparametric model by fitting both linear and nonlinear relationships between the dependent variable and multiple independent variables. One of the advantages of GAM is that it does not require prior assumptions about the correlation between independent variables. This approach offers greater flexibility in constructing relationships between dependent and explanatory variables [33]. The specific construction forms of GAM can include the types shown in Equations (3) and (4):

$$g(\mu) = f_1(X_1) + f_2(X_2) + \cdots + f_p(X_p) + \varepsilon \quad (3)$$

$$\mu = E(\frac{Y}{X_1, X_2, \cdots, X_p}) \quad (4)$$

$g(\mu)$ represents the connection function, ε is a random error term, Y refers to As content, X_p is the factor affecting As content (DOM, Fe), and f_p is the fitting relationship between As content and DOM, Fe.

2.7. Data Statistics and Analysis

Software (SPSS 27.0 and Excel) was utilized for the mathematical analysis of the data, while R Studio, Origin 2021, Matlab R2023b, and ArcGIS 10.7 were employed for mapping. Spearman correlation and semi-variance Generalized Additive Models (GAM) were used to analyze the associations between DOM components, iron (Fe), and arsenic (As), utilizing the R packages "corrplot" and "MGCV". The non-parameter test for k independent samples (Kruskal-Wallis Test) was conducted to analyze the difference of distribution of DOC, As and Fe content of soil by SPSS 20.0.

3. Results and Discussion

3.1. Physicochemical Properties of Tea Plantation Soil

The pH values of the soils in the three tea plantations of Huangshan City ranged from 3.9 to 5.2, with an average value of 4.3 ± 0.3, and the whole area was strongly acidic, which was closely related to the soil formation process. The tea plantations in Huangshan City are dominated by red soil, and the strong desilication and alumina enrichment of red soil in the soil formation process led to an increase in the exchangeable H^+ and Al^{3+} content of the soil, coupled with its weak acid buffering capacity, resulting in the soil showing strong acidity. The total carbon (TC) contents of the soils of the three tea plantations in Huangshan City ranged from 7.83 to 48.05 g·kg^{-1}, and the TC contents of the soils of the HSMF (20.14 ± 8.87 g·kg^{-1}) were higher than those of the QMH (16.84 ± 3.11 g·kg^{-1}) and the TPHK (15.53 ± 5.61 g·kg^{-1}), but there was no significant difference in the TC contents of the soils of the three tea plantations. In addition, the distribution of the soil total nitrogen (TN) content in the three tea plantations was consistent with TC, showing the distribution characteristics of HSMF (2.12 ± 0.77 g·kg^{-1}) > QMH (1.89 ± 0.30 g·kg^{-1}) > TPHK production areas (1.65 ± 0.50 g·kg^{-1}). Among them, the soil TN content of the HSMF production area was significantly higher than that of the TPHK production area (p = 0.35 < 0.05).

3.2. Soil DOC, Fe, and As Content and Correlation

The DOC content in the soils of the three tea plantations in Huangshan City ranged from 8.39 to 37.66 mg·kg^{-1}, with an average content of 16.99 ± 5.41 mg·kg^{-1} (Table S1). Among the different areas, the highest average DOC content was found in the soil of the HSMF, which exceeded 18 mg·L^{-1}, followed by the QMH (16.33 mg·kg^{-1}), and the TPHK

(15.84 mg·kg^{-1}). However, there was no significant difference in DOC contents among the three tea gardens (Figure S1a).

The average soil Fe content varied significantly across the three plantations, with the QMH (41,628 mg·kg^{-1}) showing the highest content, followed by the HSMF (37,552 mg·kg^{-1}), and the TPHK (30,181 mg·kg^{-1}) (Figure S1b). Qimen County, part of the Jiangnan uplift region of the Yangtze Plateau, has a stratigraphy dating to the Late Jurassic period during the Yanshan Movement, which caused intense geological shifts and large-scale magma intrusion. This geological activity exposed substantial Fe-containing minerals at the surface. Under the influence of the subtropical monsoon climate, desilicification and biocontent processes have resulted in significantly higher Fe content in the QMH soils compared to other areas.

The soil As content ranged from 1.70 mg·kg^{-1} to 43.85 mg·kg^{-1}, and its distribution pattern across the three tea plantations mirrored that of Fe (Figure S1c). Although the average soil As content in the three areas did not exceed the screening threshold for agricultural land soil pollution (40 mg·kg^{-1}), there was moderate variation. The average soil As content in the HSMF and QMH was 1.24 and 3.13 times higher than the regional background level, respectively. Intense human activities, such as the frequent use of fertilizers and pesticides, transportation, and mining, have released significant amounts of As into the soil, strongly influencing its spatial distribution and accumulation [25].

While the DOC content in the soil of tea plantations does not have a significant impact on Fe and As levels, the Fe content is strongly and positively correlated with the As content (r = 0.048, p < 0.001) (Figure 2). Fe oxides in the soil play a key role in the sorption and coprecipitation of As [34,35]. As can be adsorbed onto Fe oxides through ligand exchange with functional groups like -OH or through electrostatic interactions, forming complexes that immobilize As in the soil. Additionally, As can form secondary oxide compounds with Fe or coprecipitate with free Fe ions, reducing its mobility and toxicity. The higher Fe levels in the QMH soils provide more binding sites for As ions, creating favorable conditions for As fixation and explaining the elevated soil As content in this area.

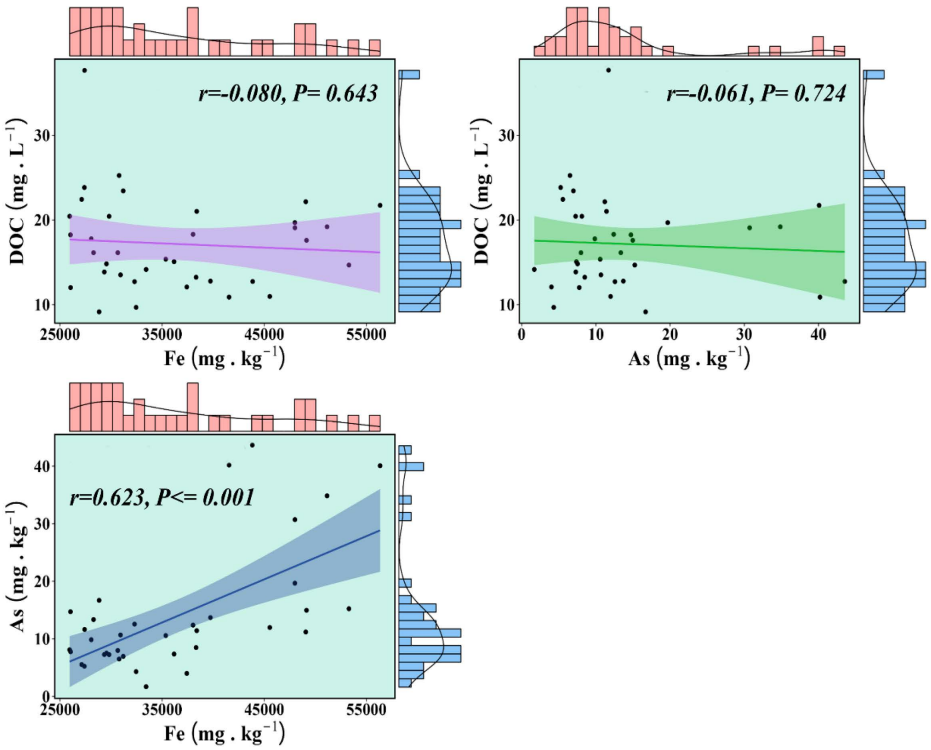

Figure 2. Linear correlation plots of DOC, Fe, and As contents of tea plantation soils. The colored area around the regression line indicates the 95% confidence interval.

3.3. Fluorescence Spectral Characteristics of DOM in Tea Plantation Soil

The average FI value of soil DOM in the tea plantations in Huangshan City was 2.04 ± 0.19, and the overall BIX value ranged from 0.7 to 1.0, indicating a strong autochthonous source of DOM (the parameter calculation methods and explanations for *FI*, *BIX*, *HIX*, and β/α are shown in Table S2 of Supplementary Materials). This suggests that endogenous metabolites generated by microbial decomposition are the primary source of DOM (Figure 3a). The strong endogenous characteristics may be linked to local farming practices. Since tea thrives in relatively poor soils, tea growers avoid using additional fertilizers, instead covering the soil with pruned tea leaves. As a result, the DOM is largely formed from the decomposition of dead leaves and branches. As shown in Figure 3b, the HIX values of soil DOM in the tea plantations were generally below 6, indicating a low degree of humification. Higher β/α values suggest a greater proportion of recent organic matter in the DOM. The β/α values of soil DOM in these tea plantations ranged from 0.64 to 0.99, with an average of 0.77 ± 0.08, which indicates a high level of biological activity in the soil. The presence of fresh DOM provides an important supplement to the soil organic matter. The frequent pruning of tea trees introduces a significant amount of fresh organic material into the soil. Additionally, the hilly slopes on which the tea plantations are located, combined with concentrated rainfall, result in substantial leaching of DOM, especially DOM with a high degree of decomposition. This contributes to the relatively high proportion of fresh DOM in the soil.

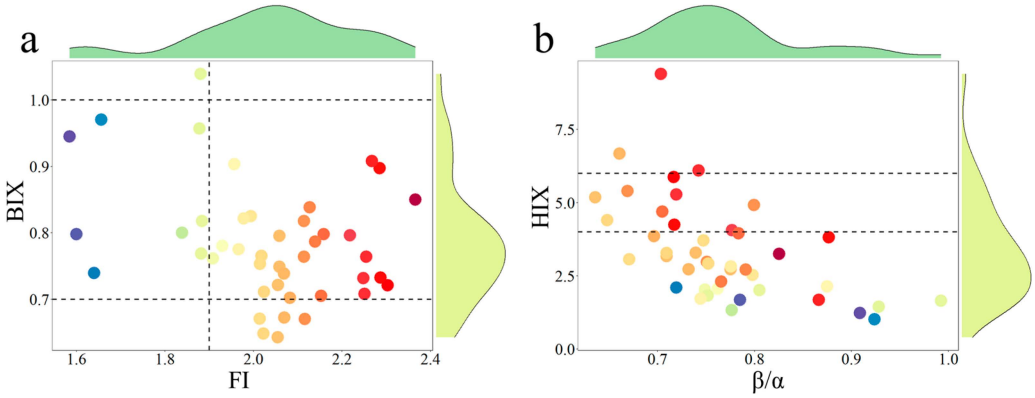

Figure 3. Distribution of fluorescence index of soil DOM in tea plantations in Huangshan City. (**a**) distribution of fluorescence index and autochthonous index; (**b**) distribution of β/α and humification indicators. FI, fluorescence index; BIX, autochthonous index; β/α, the proportion of the newborn DOM in the overall DOM; HIX, humification indicators.

Fluorescence excitation-emission matrix parallel factor analysis (EEM-PARAFAC) was used to decompose the three-dimensional fluorescence spectra of the soil DOM from tea plantations in Huangshan City. The analysis identified four distinct fluorescence fractions, with each fraction's excitation (Ex) and emission (Em) wavelengths shown in Figure 4. Component C1 (Ex/Em = 345/414 nm) is a UVA HA component with a low molecular weight, mainly formed by the decomposition of organic matter in the soil [36]. Component C2 (Ex/Em = 390/464 nm) is classified as a terrigenous humic-like component with a large molecular weight and complex molecular structure [37]. Component C3 (Ex/Em = 290(325)/338 nm) corresponds to the traditional protein-like T-peak, generally attributed to free or bound tryptophan, amino acids, and other protein-related substances [38,39]. Component C4 (Ex/Em = 390/406 nm) is considered to originate from exogenous inputs and human activities, representing hydrophobic HA components.

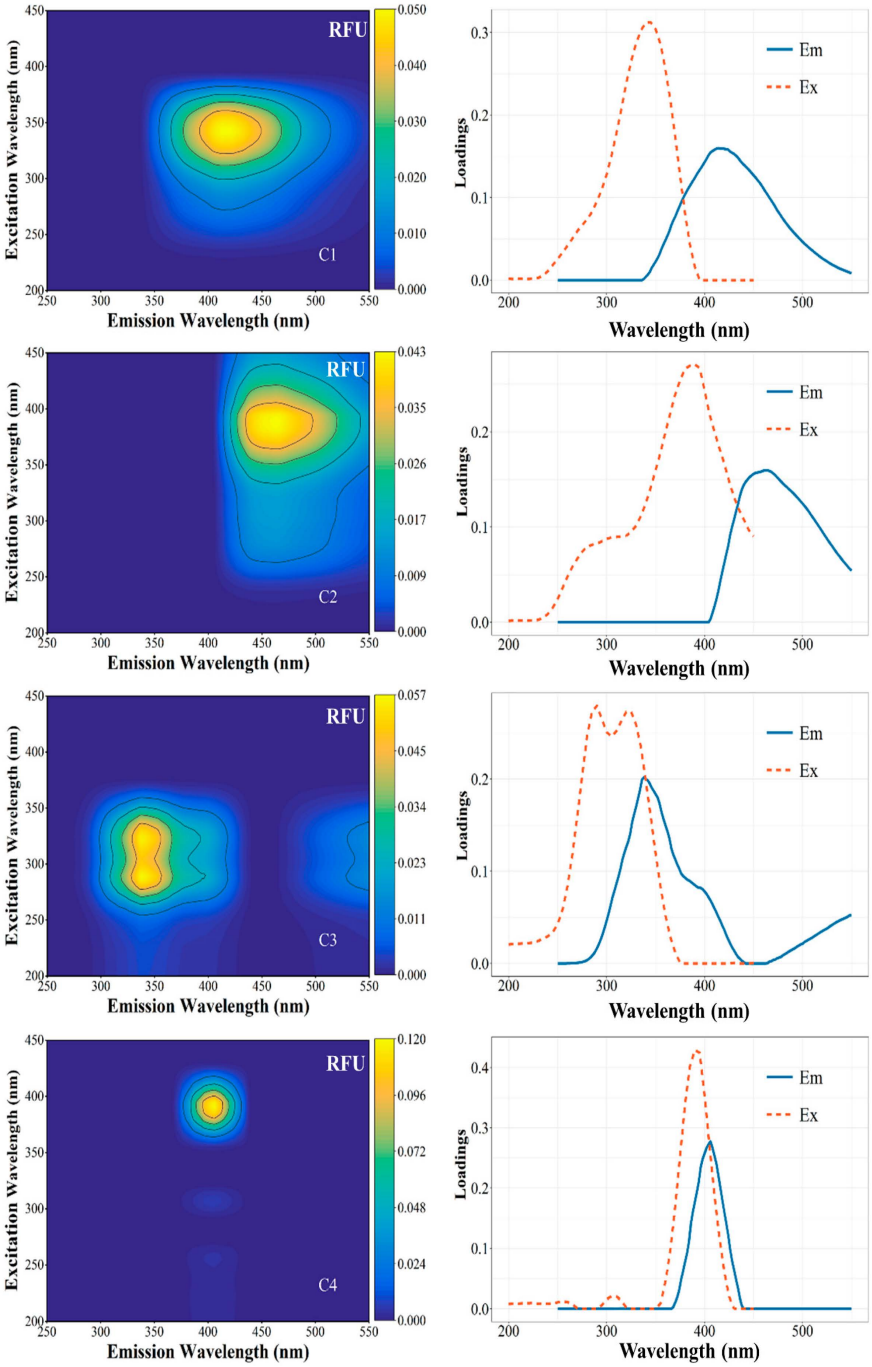

Figure 4. EEM-PARAFAC identification of spectral characteristics of DOM components. Component C1 (Ex/Em = 345/414 nm), UVA HA component. Component C2 (Ex/Em = 390/464 nm), terrigenous humic-like component. Component C3 (Ex/Em = 290(325)/338 nm), protein-like T-peak. Component C4 (Ex/Em = 390/406 nm), hydrophobic HA components.

The relative abundance of each component was calculated based on the maximum fluorescence intensity (Fmax), and the differences were compared (Figure S2). The results show that in 47% of the soil samples, the combined relative abundance of C1, C2, and C4 exceeded 90%, while the relative abundance of C3 (protein-like) averaged only 12%. This indicates that HA components dominate the soil DOM in tea plantations.

3.4. Correlation Between DOM Components and As and Fe Contents

There was no significant correlation between the As content and DOM content, composition, or structure, but a significant correlation was found between the As content and Fe content. Additionally, the Fe content was significantly correlated with the HA-like components, C1 and C2 (Figure 5a–e). The DOM and As form complexes primarily through two mechanisms. First, the DOM interacts with As via active functional groups such as -OH, -COOH, and C=O, forming complexes through ligand exchange. Second, the DOM can bind to As and its oxides, forming a ternary complex (DOM-metal-As) with the aid of a metal bridge bond [22]. Although there was no direct statistical correlation between the DOM and As, the significant correlations between Fe and both As and DOM components suggest that Fe and DOM may interact to influence soil As content.

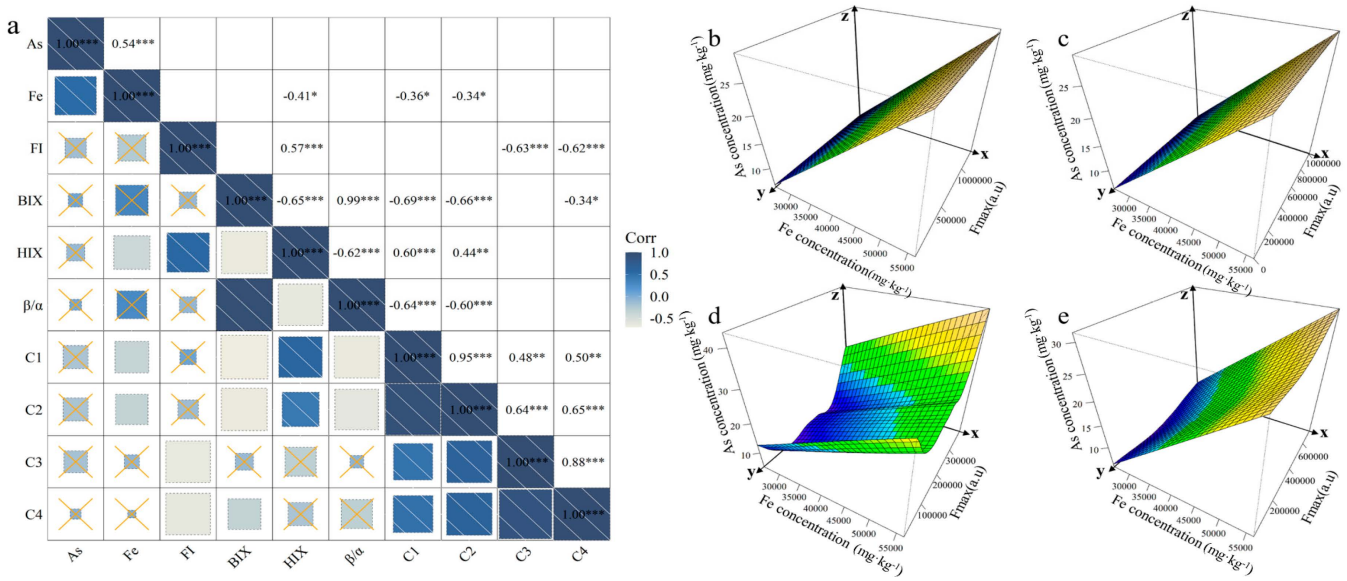

Figure 5. Correlation analyses of As and Fe with DOM fractions and spectral indices (**a**), and the effect of DOM fractions and Fe interaction on As content (**b**–**e**). The size of the squares and numbers in (**a**) indicate changes in correlation coefficients, and asterisks (*) indicate the level of significance ("*" indicates $p < 0.05$, "**" indicates $p < 0.01$, and "***" indicates $p < 0.001$). (**b**–**e**) refer to C1 ∩ Fe, C2 ∩ Fe, C3 ∩ Fe and C4 ∩ Fe, respectively. The *x*-axis is the soil Fe content, *y*-axis is the maximal fluorescence intensity of DOM fractions, and *z*-axis is the linear predictive value of As content.

The interaction between specific DOM fractions and Fe in tea garden soils had a direct impact on the distribution of As content (Table S3). Among these, the interaction between C3 (protein-like fraction) and Fe had the greatest influence on As content, followed by C4, while C1 and C2 (HA-like fractions) had smaller and equal effects. When the fluorescence intensity and Fe content of the DOM components were varied, the As content showed different response patterns (Figure 5b–e). For HA-like components (C1 and C2), the soil As content increased only as the Fe content increased, and the impact of these components on the soil As was not significant (Figure 5b,c). However, the coexistence of C3 (protein-like fraction) with Fe caused a significant increase in the soil As content, and the interaction between C3 and Fe had a far greater effect on the As content than the other DOM fractions (Figure 5d, Table S3). Specifically, when the maximum fluorescence intensity of C3 was below 100,000 RFU, the soil As content slightly decreased. As the Fe content increased and the maximum fluorescence intensity of C3 ranged from 100,000 to 300,000 RFU, the soil As content increased gradually. Once the maximum fluorescence intensity of C3 exceeded 300,000 RFU, the soil As content rose rapidly with the increased abundance of the protein-like fraction and Fe content. For C4 (hydrophobic humic-like fraction), its interaction with Fe also led to an increase in the soil As content as both C4 and Fe levels rose. However, the

Fe content had a much more pronounced effect on soil As accumulation than the humic-like component (Figure 5e).

3.5. DOM-Fe Binding Process with As

The coexistence of DOM and Fe amplifies the mobility and diffusivity of As [40]. In experiments involving only the DOM, approximately 3.94–15.45% of As in the free state diffused into the DOM pores and subsequently exhibited binding to the DOM (Figure 6a). The mobility of As is primarily influenced by the surface functional groups of the DOM [41]. Both As (III) and As(V) undergo ligand exchange with DOM surface hydroxyl groups (-OH) and, within a specific pH range, can bind to DOM -OH groups to form stable anionic complexes via the internal hydrogen bonds of the DOM [42]. When DOM coexists with Fe, the proportion of free As bound to the DOM increases significantly. At the Fe content of 1 mg·L^{-1}, the DOM-bound As ranged from 2.45% to 16.79% of total As. With Fe content increases, the proportion of As bound to DOM also rose, ranging from 4.71% to 29.04% as the Fe content increased, reaching 14.44–30.32% at the highest levels (Figure 6b). This indicates that Fe significantly enhances the DOM's ability to bind As. The ternary complex formed through the interaction of DOM, Fe, and As boosts As mobility, as Fe acts as a bridge between the negatively charged As and electronegative organic ligands, promoting the sorption of DOM to As. As the Fe content increases, more bridging bonds form, resulting in greater As-DOM binding [43,44]. Thus, higher Fe contents decrease free As in the environment and increase the amount of As bound to the DOM. Fitting the results to an isothermal sorption model revealed that the sorption of DOM-Fe to As follows the Freundlich model (Table S4), suggesting that Fe-mediated DOM-As binding occurs through heterogeneous, multi-layer sorption. The 1/n value, which was between zero and one under all conditions, indicates that DOM-Fe can effectively adsorb As [23].

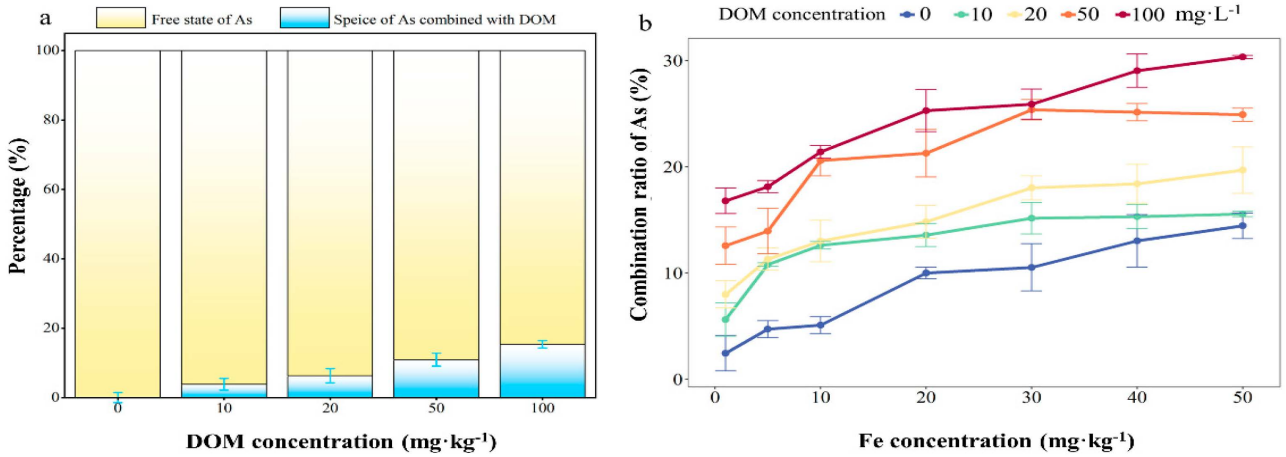

Figure 6. Combination rate of As by DOM-Fe with different content ratios. (**a**) The relative percentage of free state As and combination As in water at different DOM concentrations. (**b**) The combination ratio of DOM to As in water at different concentrations of DOM and Fe.

3.6. DOM-Fe Binding Mechanism with As

Scanning electron microscopy (SEM) was employed to further investigate the structural and morphological changes resulting from the combination of DOM-Fe with As, and the results are presented in Figure 7. The DOM-Fe conjugate displayed honeycomb-like morphological features characterized by a rough, uneven surface and a large number of irregular, loose pores (Figure 7a). However, after the combination of DOM-Fe with As, the surface of the resulting ternary complex became flat and smooth, with many of the original loose pores filled in and more crystal-like structures attached to the surface (Figure 7b). The pore structure significantly affects the sorption capacity of organic ligands for metal ions, with more pronounced pore structures allowing for greater metal ion sorption [45]. The complex pore structure on the surface of the DOM-Fe compound provides numerous

sorption sites [46]. When As is introduced into the system, the loose pore structure on the surface of the DOM-Fe compound disappears, replaced by a smooth surface. This suggests that As is complexed with DOM-Fe via these pores, leading to the disappearance of the porous structure and the formation of a more compact complex.

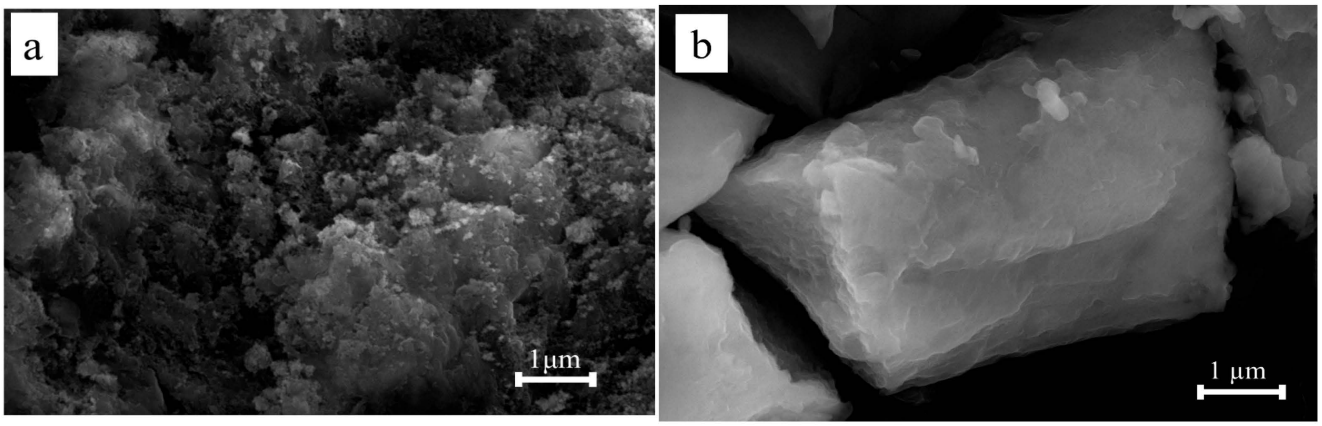

Figure 7. SEM images of DOM-Fe before and after bonding with As ((**a**) before bonding; (**b**) after bonding).

Before binding to As, the surface of the DOM-Fe complex was predominantly composed of carbon (C) and oxygen (O), with normalized masses of 67.62% and 30.56%, respectively, while the Fe occupied a smaller portion, only 1.82% (Table S5). The elemental distribution of the DOM-Fe surface showed that C, O, and Fe were uniformly distributed, indicating that the Fe was evenly adsorbed across the surface. After binding with As, the relative mass of C on the DOM-Fe complex increased, although there was less surface adhesion. The oxygen content showed no significant change, but the Fe became scattered, and its normalized mass decreased drastically to just 0.01% on the surface of the complex (Table S5). This indicated that the DOM-Fe complexes were able to promote the combination of As through surface pore adsorption, electrostatic interactions, and the action of surface functional groups. Research indicates that Fe(citrate) acts as an electron acceptor, promoting the binding between the DOM and As [47,48]. As ions, attracted by Fe due to charge differences after entering the DOM-Fe system, are adsorbed onto the Fe surface, this leads to Fe on the surface of the complex being covered by As [20,49,50].

4. Conclusions

The DOM of the red soil of the tea plantations in Huangshan City has strong endogenous properties and a low degree of humification. EEM-PARAFAC analysis was used to extract four DOM fractions from the Fe-rich tea garden soil, including three HA-like fractions (C1, C2, and C4) and one protein-like fraction (C3), with a higher relative abundance of HA-like fractions. The DOC content in the Fe-rich red soil was not directly correlated with either Fe or As, but the significant correlation of DOM fractions with Fe ($r = -0.36$, $p < 0.05$; $r = -0.34$, $p < 0.05$) and Fe with As ($r = 0.54$, $p < 0.001$) implies that DOM is able to bind to As with the involvement of Fe. The soil As content would increase in parallel with the relative abundance of the four DOM fractions and Fe content, but the effect of protein-like fractions interacting with Fe on the As content was more pronounced. The sorption of As by HA was enhanced by 49% to 75% with the participation of Fe. This indicates that Fe, as a metal electronic bridge, improves the binding ability of DOM to As. DOM-Fe compounds bind As through surface pores and functional groups. These findings will add to the current understanding of As environmental behavior driven by DOM and Fe and provide insights for the study of As pollution control in red soil tea plantations.

Supplementary Materials: The following supporting information can be downloaded at: https://www.mdpi.com/article/10.3390/agriculture14122289/s1, Table S1: Descriptive statistics of DOC, Fe, and As content of tea plantation soils; Table S2: Characterization of dissolved organic matter by spectral analysis; Table S3: Fitting parameters for As, Fe, and DOM component interactions based on GAM modeling; Table S4: Parameters of isotherm model fitting for As sorption by DOM-Fe; Table S5: Normalized mass of each element on the surface of DOM-Fe before and after combining with As; Figure S1: Soil DOC (a), Fe (b), and As (c) contents and their differences in different tea plantations; Figure S2: Maximum fluorescence intensity maps of four fractions in the soil DOM of tea plantations.

Author Contributions: Conceptualization, Y.Y., J.Y. and F.F.; methodology, Y.Y., J.L. and J.Z.; software, K.M.; validation, Y.L. and H.T.; formal analysis, Y.Y.; investigation, Y.Y., J.Z. and H.T.; resources, F.F.; data curation, J.L. and J.Y.; writing—original draft preparation, Y.Y.; writing—review and editing, J.Y. and F.F.; visualization, K.M.; supervision, Y.Y.; project administration, F.F.; funding acquisition, Y.Y. and Y.L. All authors have read and agreed to the published version of the manuscript.

Funding: This work was supported by the National Natural Science Foundation of China (Grant Nos. 42207454, 42471088).

Institutional Review Board Statement: Not applicable.

Data Availability Statement: Data will be made available on request.

Conflicts of Interest: The authors declare no conflicts of interest.

References

1. Rehman, M.U.; Khan, R.; Khan, A.; Qamar, W.; Arafah, A.; Ahmad, A.; Ahmad, A.; Akhter, R.; Rinklebe, J.; Ahmad, P. Fate of arsenic in living systems: Implications for sustainable and safe food chains. *J. Hazard. Mater.* **2021**, *417*, 126050. [CrossRef] [PubMed]
2. Wu, M.; Qi, C.; Derrible, S.; Choi, Y.; Fourie, A.; Ok, Y.S. Regional and global hotspots of arsenic contamination of topsoil identified by deep learning. *Commun. Earth Environ.* **2024**, *5*, 10. [CrossRef]
3. Li, Y.Y.T.; Zhang, Y.L.; Chen, J.Y.; Yang, G.F.; Li, H.H.; Wang, J.J.; Li, W.Y. Ecological risk assessment and source analysis of heavy metals in farmland soil in Yangchun city based on APCS-MLR and geostatistics. *Agriculture* **2024**, *14*, 309. [CrossRef]
4. Huang, Y.; Wang, L.; Wang, W.; Li, T.; He, Z.; Yang, X. Current status of agricultural soil pollution by heavy metals in China: A meta-analysis. *Sci. Total Environ.* **2019**, *651*, 3034–3042. [CrossRef]
5. Gong, Y.; Qu, Y.; Yang, S.; Tao, S.; Shi, T.; Liu, Q.; Chen, Y.; Wu, Y.; Ma, J. Status of arsenic accumulation in agricultural soils across China (1985–2016). *Environ. Res.* **2020**, *186*, 109525. [CrossRef]
6. Zhang, S.; Zhang, J.; Niu, L.; Chen, Q.; Zhou, Q.; Xiao, N.; Man, J.; Ma, J.; Wei, C.; Zhang, S.; et al. Escalating arsenic contamination throughout Chinese soils. *Nat. Sustain.* **2024**, *7*, 766–775. [CrossRef]
7. Upadhyay, M.K.; Shukla, A.; Yadav, P.; Srivastava, S. A review of arsenic in crops, vegetables, animals and food products. *Food Chem.* **2019**, *276*, 608–618. [CrossRef]
8. Zhang, T.; Zheng, B.; Wang, M.; He, J.; Xia, S. Spatial distribution, occurrence form, availability and ecological risk assessment of arsenic in soils of riparian zones on the Tibetan Plateau. *Gondwana Res.* **2024**, *130*, 131–139. [CrossRef]
9. Byeon, E.; Kang, H.-M.; Yoon, C.; Lee, J.-S. Toxicity mechanisms of arsenic compounds in aquatic organisms. *Aquat. Toxicol.* **2021**, *237*, 105901. [CrossRef]
10. Wang, J.; Li, Z.; Zhu, Q.; Wang, C.; Tang, X. Review on arsenic environment behaviors in aqueous solution and soil. *Chemosphere* **2023**, *333*, 138869. [CrossRef]
11. Cao, H.Z.; Bu, F.Y.; Li, X.D.; Liu, W.X.; Sun, Z.Q.; Shen, J.L.; Ma, F.J.; Gu, Q.B. Unravelling structure evolution of dissolved organic matter during oxidation by persulfate: Insights from aromaticity and fluorescence analysis. *Environ. Res.* **2024**, *259*, 119518. [CrossRef] [PubMed]
12. Zhang, F.; Zhang, H.; Wu, Y.; Xiao, Y.; Huang, W.; Tang, J.; Yuan, Y.; Chen, J.B. Inhibiting effects of humic acid on iron flocculation hindered As removal by electro-flocculation on air cathode iron anode. *Ecotoxicol. Environ. Saf.* **2024**, *275*, 116228. [CrossRef] [PubMed]
13. Hao, C.; Sun, X.; Peng, Y.; Xie, B.; He, K.; Wang, Y.; Liu, M.; Fan, X. Geochemical impact of dissolved organic matter on antimony mobilization in shallow groundwater of the Xikuangshan antimony mine, Hunan Province, China. *Sci. Total Environ.* **2023**, *860*, 160292. [CrossRef] [PubMed]
14. Li, D.; Chang, F.; Zhang, Y.; Duan, L.; Liu, Q.; Li, H.; Hu, G.; Zhang, X.; Gao, Y.; Zhang, H. Arsenic migration at the sediment-water interface of anthropogenically polluted Lake Yangzong, Southwest China. *Sci. Total Environ.* **2023**, *879*, 163205. [CrossRef]
15. Abdelrady, A.; Sharma, S.; Sefelnasr, A.; Kennedy, M. Characterisation of the impact of dissolved organic matter on iron, manganese, and arsenic mobilisation during bank filtration. *J. Environ. Manag.* **2020**, *258*, 110003. [CrossRef]

16. Jiang, J.; Wang, X.; Su, C.; Wang, M.; Ren, F.; Huq, E. Unraveling the impact of dissolved organic matter on arsenic mobilization in alluvial aquifer of the lower Yellow River basin, Northern China. *Appl. Geochem.* **2023**, *158*, 105781. [CrossRef]
17. He, S.; Wang, X.; Zheng, C.; Yan, L.; Li, L.; Huang, R.; Wang, H. Enhanced arsenic depletion by rice plant from flooded paddy soil with soluble organic fertilizer application. *Chemosphere* **2020**, *252*, 126521. [CrossRef]
18. Zhang, F.; Li, X.; Duan, L.; Zhang, H.; Gu, W.; Yang, X.; Li, J.; He, S.; Yu, J.; Ren, M. Effect of different DOM components on arsenate complexation in natural water. *Environ. Pollut.* **2021**, *270*, 116221. [CrossRef]
19. Qian, G.; Xu, L.; Li, N.; Wang, K.; Qu, Y.; Xu, Y. Enhanced arsenic migration in tailings soil with the addition of humic acid, fulvic acid and thiol-modified humic acid. *Chemosphere* **2022**, *286*, 131784. [CrossRef]
20. Qiao, W.; Guo, H.; He, C.; Shi, Q.; Zhao, B. Unraveling roles of dissolved organic matter in high arsenic groundwater based on molecular and optical signatures. *J. Hazard. Mater.* **2021**, *406*, 124702. [CrossRef]
21. Hoffmann, M.; Mikutta, C.; Kretzschmar, R. Arsenite binding to natural organic matter: Spectroscopic evidence for ligand exchange and ternary complex formation. *Environ. Sci. Technol.* **2013**, *47*, 12165–12173. [CrossRef] [PubMed]
22. Yao, Y.; Mi, N.; He, C.; Yin, L.; Zhou, D.; Zhang, Y.; Sun, H.; Yang, S.; Li, S.; He, H. Transport of arsenic loaded by ferric humate colloid in saturated porous media. *Chemosphere* **2020**, *240*, 124987. [CrossRef] [PubMed]
23. Aftabtalab, A.; Rinklebe, J.; Shaheen, S.M.; Niazi, N.K.; Moreno-Jimenez, E.; Schaller, J.; Knorr, K.H. Review on the interactions of arsenic, iron (oxy)(hydr)oxides, and dissolved organic matter in soils, sediments, and groundwater in a ternary system. *Chemosphere* **2022**, *286*, 131790. [CrossRef] [PubMed]
24. Solgi, E.; Esmaili-Sari, A.; Riyahi-Bakhtiari, A.; Hadipour, M. Soil contamination of metals in the three industrial estates, Arak, Iran. *Bull. Environ. Contam. Toxicol.* **2012**, *88*, 634–638. [CrossRef]
25. Zhang, J.; Yang, R.; Chen, R.; Peng, Y.; Wen, X.; Gao, L. Accumulation of heavy metals in tea leaves and potential health risk assessment: A Case study from Puan County, Guizhou Province, China. *Int. J. Environ. Res. Public Health* **2018**, *15*, 133. [CrossRef]
26. Huang, J.; Wu, Y.; Li, Y.; Sun, J.; Xie, Y.; Fan, Z. Do trace metal(loid)s in road soils pose health risks to tourists? A case of a highly-visited national park in China. *J. Environ. Sci.* **2022**, *111*, 61–74. [CrossRef]
27. Tao, C.; Song, Y.; Chen, Z.; Zhao, W.; Ji, J.; Shen, N.; Ayoko, G.A.; Frost, R.L. Geological load and health risk of heavy metals uptake by tea from soil: What are the significant influencing factors? *Catena* **2021**, *204*, 105419. [CrossRef]
28. Zhang, J.M.; Ge, W.; Xing, C.; Liu, Y.; Shen, X.F.; Zhao, B.; Chen, X.Y.; Xu, Y.P.; Zhou, S.B. Ecological risk assessment of potentially toxic elements in selenium-rich soil with different land-use types. *Environ. Geochem. Health* **2023**, *45*, 5323–5341. [CrossRef]
29. Zhao, M.S.; Qiu, S.Q.; Wang, S.H.; Li, D.C.; Zhang, G.L. Spatial-temporal change of soil organic carbon in Anhui Province of East China. *Geoderma Reg.* **2021**, *26*, e00415. [CrossRef]
30. LoRusso, N.A.; Bailey, S.W.; Zeng, T.; Montesdeoca, M.; Driscoll, C.T. Dissolved organic matter dynamics in reference and calcium silicate-treated watersheds at Hubbard Brook Experimental Forest, NH, USA. *J. Geophys. Res.-Biogeosci.* **2021**, *126*, e2021JG006352. [CrossRef]
31. Cui, H.-Y.; Zhang, S.-B.; Zhao, M.-Y.; Zhao, Y.; Wei, Z.-M. Parallel faction analysis combined with two-dimensional correlation spectroscopy reveal the characteristics of mercury-composting-derived dissolved organic matter interactions. *J. Hazard. Mater.* **2020**, *384*, 121395. [CrossRef] [PubMed]
32. Guo, X.; Xie, X.; Liu, Y.; Wang, C.; Yang, M.; Huang, Y. Effects of digestate DOM on chemical behavior of soil heavy metals in an abandoned copper mining areas. *J. Hazard. Mater.* **2020**, *393*, 122436. [CrossRef] [PubMed]
33. Pan, B.; Qiu, M.; Wu, M.; Zhang, D.; Peng, H.; Wu, D.; Xing, B. The opposite impacts of Cu and Mg cations on dissolved organic matter-ofloxacin interaction. *Environ. Pollut.* **2012**, *161*, 76–82. [CrossRef] [PubMed]
34. Hastie, T.; Tibshirani, R. Exploring the nature of covariate effects in the proportional hazards model. *Biometrics* **1990**, *46*, 1005–1016. [CrossRef]
35. Xu, X.; Chen, C.; Wang, P.; Kretzschmar, R.; Zhao, F.-J. Control of arsenic mobilization in paddy soils by manganese and iron oxides. *Environ. Pollut.* **2017**, *231*, 37–47. [CrossRef]
36. Cai, X.; Yin, N.; Liu, X.; Wang, P.; Du, H.; Cui, Y.; Hu, Z. Biogeochemical processes of arsenic transformation and redistribution in contaminated soils: Combined effects of iron, sulfur, and organic matter. *Geoderma* **2022**, *422*, 115948. [CrossRef]
37. Gao, J.; Liang, C.; Shen, G.; Lv, J.; Wu, H. Spectral characteristics of dissolved organic matter in various agricultural soils throughout China. *Chemosphere* **2017**, *176*, 108–116. [CrossRef]
38. Cui, H.-Y.; Zhao, Y.; Chen, Y.-N.; Zhang, X.; Wang, X.-Q.; Lu, Q.; Jia, L.-M.; Wei, Z.-M. Assessment of phytotoxicity grade during composting based on EEM/PARAFAC combined with projection pursuit regression. *J. Hazard. Mater.* **2017**, *326*, 10–17. [CrossRef]
39. Murphy, K.R.; Stedmon, C.A.; Waite, T.D.; Ruiz, G.M. Distinguishing between terrestrial and autochthonous organic matter sources in marine environments using fluorescence spectroscopy. *Mar. Chem.* **2008**, *108*, 40–58. [CrossRef]
40. Yao, Y.; Li, Y.-Z.; Guo, X.-J.; Huang, T.; Gao, P.-P.; Zhang, Y.-P.; Yuan, F. Changes and characteristics of dissolved organic matter in a constructed wetland system using fluorescence spectroscopy. *Environ. Sci. Pollut. Res.* **2016**, *23*, 12237–12245. [CrossRef]
41. Yao, Y.; Ma, K.; Li, S.; Zhang, Y.; Zhang, Z.; Fang, F.; Lin, Y.; Yin, L.; Sun, L.; Zhang, C. Dissolved organic matter and Fe/Mn enhance the combination and transformation of As in Lake Chaohu Basin. *J. Environ. Manag.* **2024**, *349*, 119425. [CrossRef] [PubMed]
42. Xu, Y.; Wang, K.; Zhou, Q.; Zhang, L.; Qian, G. Effects of humus on the mobility of arsenic in tailing soil and the thiol-modification of humus. *Chemosphere* **2020**, *259*, 127403. [CrossRef] [PubMed]

43. Buschmann, J.; Kappeler, A.; Lindauer, U.; Kistler, D.; Berg, M.; Sigg, L. Arsenite and arsenate binding to dissolved humic acids: Influence of pH, Type of humic acid, and aluminum. *Environ. Sci. Technol.* **2006**, *40*, 6015–6020. [CrossRef] [PubMed]
44. Lenoble, V.; Dang, D.H.; Cazalet, M.L.; Mounier, S.; Pfeifer, H.R.; Garnier, C. Evaluation and modelling of dissolved organic matter reactivity toward AsIII and AsV—Implication in environmental arsenic speciation. *Talanta* **2015**, *134*, 530–537. [CrossRef] [PubMed]
45. Rashid, M.; Sterbinsky, G.E.; Pinilla, M.Á.G.; Cai, Y.; O'Shea, K.E. Kinetic and mechanistic evaluation of inorganic arsenic species adsorption onto humic acid grafted magnetite nanoparticles. *J. Phys. Chem. C* **2018**, *122*, 13540–13547. [CrossRef]
46. Liao, W.; Zhang, X.; Ke, S.; Shao, J.; Yang, H.; Zhang, S.; Chen, H. Effect of different biomass species and pyrolysis temperatures on heavy metal adsorption, stability and economy of biochar. *Ind. Crops Prod.* **2022**, *186*, 115238. [CrossRef]
47. Zhou, L.; Zhang, Y.; Wang, Q.; Ferronato, C.; Yang, X.; Chovelon, J.M. Photochemical behavior of carbon nanotubes in natural waters: Reactive oxygen species production and effects on •OH generation by Suwannee River fulvic acid, nitrate, and Fe (III). *Environ. Sci. Pollut. Res.* **2016**, *23*, 19520–19528. [CrossRef]
48. Huang, D.Y.; Zhuang, L.; Cao, W.D.; Xu, W.; Zhou, S.G.; Li, F.B. Comparison of dissolved organic matter from sewage sludge and sludge compost as electron shuttles for enhancing Fe(III) bioreduction. *J. Soils Sediments* **2010**, *10*, 722–729. [CrossRef]
49. Liu, G.L.; Fernandez, A.; Cai, Y. Complexation of arsenite with humic acid in the presence of ferric iron. *Environ. Sci. Technol.* **2011**, *45*, 3210–3216. [CrossRef]
50. Li, X.M.; Guo, H.M.; Zheng, H.; Xiu, W.; He, W.; Ding, Q. Roles of different molecular weights of dissolved organic matter in arsenic enrichment in groundwater: Evidences from ultrafiltration and EEM-PARAFAC. *Appl. Geochem.* **2019**, *104*, 124–134. [CrossRef]